

Research Article

Evaluation of Comparative Performance of Three Wind Turbine Rotors

Basharat Salim and Mahir Es-Saheb

Mechanical Engineering Department, College of Engineering, King Saud University,
P.O. Box 800, Riyadh 11421, Saudi Arabia

Abstract: This study presents the performance evaluation of wind turbine implementing the mathematical model based on Blade Element Momentum (BEM) theory. The investigation concentrates on the comparison of power producing characteristics of three types of rotors for a horizontal axis wind turbine. The rotors considered have rectangular plan form shape with sections fabricated from aerofoil sections of NACA families. The three families of NACA airfoils used in this investigation are NACA4424, NACA23024 and NACA62-206. The lift and drag characteristics, of the rotors were experimentally obtained using 250 mm span and 60 mm chord rotor blades in an Armfield 300×300 mm subsonic, suction type and closed jet wind tunnel. The wind speeds used in the investigation were in the range of 8 to 11 m/s, which is the range of wind speeds found near the coastal belt and the mountainous parts of Saudi Arabia. Three bladed rotor subscale models of the wind turbines rotors having 250 mm rotor diameter, 100 mm blade span and 30 mm chord were used for testing rotational behavior of the wind turbines in a Plinth 600×600 mm blow down wind tunnel facility. The parameters used for the comparison in this study include variations in setting angle, diameters, tip speed ratio, taper, wind speed and angle of attack. It is observed that rotors with NACA4424 aerofoil sectioned blades produce more power at lower wind speeds and lower angles of attack where as rotors with NACA23024 aerofoil sectioned blades generate better performance at higher wind speeds and higher angles of attack. Further the taper of the rotors produced more decrease in the mass of the rotors than the decrease power produced by these. The reduction in mass could drastically decrease the inertia of the rotors which could result in higher rotational motions. Results depict the dependence of power produced on the C_d/C_l characteristics of the rotors.

Keywords: Blade element momentum theory, fluid dynamics design, wind power, wind turbines

INTRODUCTION

Wind power has the greatest future prospects among all the types of renewable and sustainable energy technologies. The leading energy conversion method for wind energy is the Horizontal Axis Wind Turbine (HAWT). This type of wind turbine makes use of propeller blades with aerofoil cross sections and implements the aerodynamic theories for its performance evaluation. Wind energy applications have rapidly increased in the world, so the efficiency of wind energy constructions are getting important. The wind energy conversion efficiency of the modern horizontal axis wind turbines is about 45% whereas the theoretical maximum value is 59.2% (Singh *et al.*, 2012). These turbines have been used for both high speeds and low speeds. Singh *et al.* (2012) and Ameku *et al.* (2008) have demonstrated that maximum benefit of wind at low wind speeds can be obtained by using rotors with thinner aerofoil sections which have cut in speeds in the range of 2-3 m/s. Renewable energy is abundant and its technologies are well established to provide complete

security of energy supply. The world wide wind energy output reached 215 TW at the end of 2011 out of this 18 TW were added only in last six months of 2011, (Renewable Energy World, 2011). This improvement has been solely due to improvements in the rotor design. The improvements have been both on aerodynamic and material fronts. Fiberglass-Reinforced Plastics material is being commonly used in the wind turbine rotors. Stealth blades having coating of RAM (glass-reinforced epoxy and plastic foam) have been build to decrease weight and inertia of the rotors. This also takes care of some of the environmental problems of the wind turbines. Besides being thin these rotors have smaller cut in speeds which can make these useful for low wind areas of the world, (Cameron, 2011). The second most improvement has been the design of special forms of aerofoils for the wind rotors such as NREL profiles (Tangler, 2000), for higher wind speeds and low Reynolds number aerofoil section technology, (Singh *et al.*, 2012; Ameku *et al.*, 2008), for lower wind speeds. The use of wind energy can minimize the consumption of resources of non-

Corresponding Author: Basharat Salim, Mechanical Engineering Department, College of Engineering, King Saud University,
P.O. Box 800, Riyadh 11421, Saudi Arabia

This work is licensed under a Creative Commons Attribution 4.0 International License (URL: <http://creativecommons.org/licenses/by/4.0/>).

renewable energy that can be preserved for future. The efforts need to be made so that the use of wind energy is optimized in the countries where normal wind blows slowly and the population is living in distant areas away from the main power grid. Further use of off shore locations can be used to maximize the output of wind turbines as the wind speed in these area is more than that at the shore or the inland locations. Many countries, (Pinto, 2011), are utilizing this option to counter act the prices of fossil fuels and their effects on the environment.

The basic theory of the horizontal wind turbine is based on modified propeller theory by Glauert (1926). Other type of wind rotor is of vertical axis type, such as Savonius rotor, (Fujisawa and Goto, 1994), which makes use of the Bernoulli dynamic pressure effect whereas the cross-flow rotor, (Shimizu *et al.*, 1998), makes use of the momentum exchange effect. The mathematical model most frequently used for horizontal wind turbine is the one based on the (BEM) blade element momentum theory. Dixon and Hall (2010), Buhl (2005) and Lindenburg (2003) have shown the process of combination of momentum, energy and blade element theories to arrive at the BEM theory for wind turbine. With the implementation of this model it is possible to design the rotor, choose the geometric characteristics of the turbine, rotor diameter, aerodynamic airfoils, chord, pitch, twist and to evaluate the forces acting on the blades so as to evaluate the power at the rotor shaft for wide range of wind velocities. In recent years this theory has been optimized and modified by Gigue`re and Selig (1999), Varol *et al.* (2001) and Gigue`re *et al.* (1999) to provide increasingly accurate results with different geometries and shapes of the horizontal axis wind turbines. This type of wind turbine is expected to have superior characteristics with a high efficiency conversion performance at high blade rotational speeds rates owing to use of the rotors with aerofoil sections. Hansen (2000) has investigated aerodynamic performance characteristics of the horizontal axis wind turbine theoretically by combining momentum, energy and blade element theory by means of the strip element method and experimentally by the use of a subscale model. Three types of blades were examined for the free stream velocity that varied from 0.8 to 4.5 m/s. The tests were carried out in open-type wind tunnel with an outlet duct diameter of 0.88 m. The blades consisted of a combination of tapered rectangular NACA44 and LS04 aerofoil series blades and two-stage pitch angle tapered blades from the NACA44 series. The power and torque coefficients of the wind turbine were related with the tip speed ratio both experimentally and analytically. It may be added here that the aerofoil performance of a horizontal axis wind turbine like any other wind machine is determined by the aerodynamic characteristics of the rotors. Lanzafame and Massina

(2007), Lanzafame and Massina (2009), Ozgener (2005) and Ozgener (2006) have demonstrated the effect of various mechanical and aerodynamic parameters on optimization of power output from horizontal axis wind turbines under different conditions.

The investigation concerning wind turbines has been carried out in two directions. The first has been purely aerodynamic nature which uses the wind tunnel tests, energy, momentum and blade element theories for the design analysis of the turbines. These investigations, like (Tangler, 2000; Glauert, 1926; Buhl, 2005), basically use aerodynamics for the design improvements of the wind turbine rotors. Another aspect of wind energy research is focused on availability of wind energy at a location based on energy analysis of the wind turbine rotors. These investigations, like (Burton *et al.*, 2001; Lanzafame and Massina, 2007; Ozgener, 2007), use thermodynamic analysis of the existing wind rotors for their performance optimization based on energy availability and economic considerations. Ozgener and Ozgener (2007) have coupled energy and energy analysis for a small wind energy generator. Rope *et al.* (2010), Sahin *et al.* (2006) and Baskut *et al.* (2010) are some of examples of research carried out on the exergical meteorological, environmental and reliability aspects of the wind energy.

This investigation addresses the aerodynamic performance evaluation of wind turbine rotors. A particular emphasis has been given to the measurement of the aerodynamic characteristics of the wind turbine rotor. Three shapes of rotors made out of NACA4424, NACA23024 and NACA62-206 aerofoil sections have been tested for obtaining their aerodynamic and rotational characteristics. Two hundred and fifty millimeter span blade models, of each aerofoil section, have been used for aerodynamic testing in a 300×300 mm suction type wind tunnel where as three 225 mm rotor diameter subscale wind turbine rotor models were used for obtaining rotational behavior of the rotors in a 600×600 mm blow down wind tunnel. These aerodynamic and rotational characteristics have been used for the parametric study of performance evaluation of wind turbines. The selected parameters for the parametric study include variations in setting angle, diameters, tip speed ratio, taper, wind speed and angle of attack.

MATHEMATICAL MODEL

The mathematical model used by designers is based on blade element momentum theory as discussed by Dixon and Hall (2010), Koki *et al.* (2005) and Lanzafame and Massina (2007). This theory has been utilized to perform design and performance analysis of

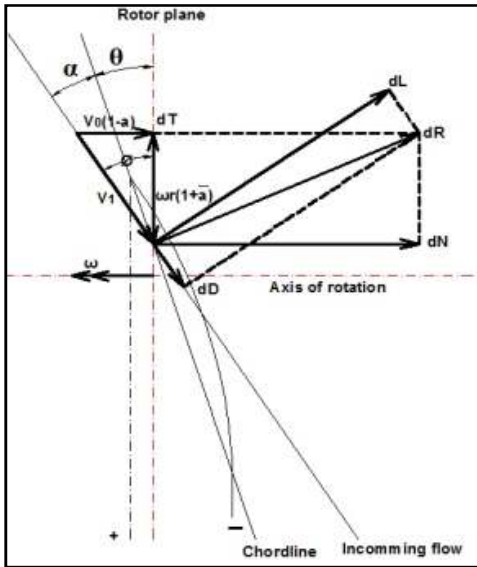


Fig. 1: Velocity and forces on an aerofoil section of a wind rotor



Fig. 2: Lift and drag measurement on 300 mm aerofoil model in Arms field 300x300 mm subsonic wind tunnel

rotors and find the geometrical variations of wind turbine rotors based on aerodynamic consideration. This theory uses energy, momentum and blade element principles to evaluate the torque and power produced by the wind turbine rotors. Figure 1 shows the aerofoil section of a wind rotor lying between radii r and $r + dr$. In reckoning the velocity of the blade element relative to the fluid consists of the free stream velocity V_0 and the rotational velocity ωr . As the rotor rotates an additional axial inflow occurs near the rotor that changes the axial velocity V_0 to $V_0(1-a)$. Similarly the additional rotational inflow makes the rotational velocity as $\omega r(1+a')$, where a and a' are the axial inflow factor and rotational inflow factor respectively. The total velocity becomes V_1 which is the vectorial sum of axial and rotational velocity components. The figure also shows components of velocity and force vectors on it. The normal and tangential forces that act on the blade section of the rotor are depicted as dN and dT , respectively. The resultant of the sectional forces

and its components in vertical and horizontal directions are indicated as dR , dL and dD , respectively. The power generated by the rotor is given by the following equation (Koki *et al.*, 2005):

$$P = \frac{\rho}{2} \omega Z \int_{R_h}^{R_t} V_1^2 c(r) (C_L \sin(\phi) - C_D \cos(\phi)) r dr$$

where, the velocity component V_1 is given as:

$$V_1^2 = V_0^2(1-a)^2 + \omega^2 r^2(1+a')^2$$

where, a and a' have been calculated using the methods given by Dixon and Hall (2010) and Lanzafame and Massina (2007). The various relations involved in the calculation of the induction factors are:

$$\frac{a}{1-a} = \frac{\lambda'(\cos(\phi) + \epsilon \sin(\phi))}{F \sin^2(\phi)}$$

$$\frac{a'}{1-a'} = \frac{\lambda'(\sin(\phi) - \epsilon \cos(\phi))}{F \sin(\phi) \cos(\phi)}$$

where, F and λ are given as:

$$F = \frac{2}{\pi} \cos^{-1} \left(e^{-\frac{\pi d}{s}} \right)$$

$$s = \frac{2\pi R_t}{Z} \sin(\phi)$$

$$d = R_t - R_h$$

$$\lambda' = \frac{Zc(r)C_L}{8\pi R_m}$$

$$R_m = \frac{R_t + R_h}{2}$$

$$\epsilon = \frac{C_d}{C_l}$$

DESCRIPTION OF EXPERIMENTAL SETUP

The basic aerodynamic characteristics lift and drag coefficients, of the rotors were experimentally obtained by testing rotor models of 250 mm span and 60 mm chord, Fig. (2), in a Arms field 300x300 mm subsonic, suction type and closed jet wind tunnel using its wind tunnel balance. Three models for the three aerofoil sections were fabricated as per the model specification of the tunnel. The wooden models used for obtaining aerodynamic characteristics were fabricated on CNC laser cutting machine. The aerofoils were fabricated by fixing skin over the aerofoil webs made by laser cutting machine. The wind speeds used were in the range of 8 to 11 m/s, which is the range of wind speeds found near the coastal belt and the mountainous parts of the



Sub scale model and plinth 600x600 mm subsonic wind tunnel



NACA62-206

NACA23024

NACA4424

Aerofoil sections of sub scale models

Fig. 3: Sub scale models in plinth 600x600 mm subsonic wind tunnel

Saudi Arabia. The rotational behavior of the wind turbines was tested by using three bladed 250 mm diameter rotor of 100 mm rotor span and 30 mm chord subscale models, Fig. (3), in a Plinth 600×600 mm blow down wind tunnel facility. The models were placed in the wind tunnel test section. The lift and drag on the models was measured with the help of the wind tunnel balance where as the rotational speed of subscale models were measured by using flashing stroboscope. Tests were carried out at Reynolds numbers ranging from 0.31×10^5 to 0.42×10^5 . The uncertainties of velocity lift coefficient and drag coefficient were calculated using ASME methodology, (Moffat, 1985) and the analysis is given in Appendix. The values of uncertainty for wind velocity lift coefficient and drag coefficient are 0.8, 1.2 and 4.2%, respectively.

RESULTS AND DUSCUSSIONS

The aerodynamic and rotational characteristics of main models and subscale models respectively were measured. Based on these results an assessment of the power producing capability of three wind turbine rotors with variations in the basic geometrical and performance parameters was carried out.

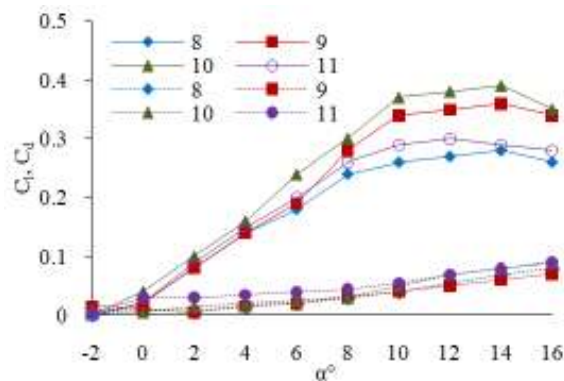


Fig. 4: Variation of lift and drag coefficient with angle of attack for NACA-62-206 airfoil

Aerodynamic characteristics: The airfoil is one of the fundamental parts of a rotor blade design. Its purpose is to induce suction on the upper surface of the blade to generate lift. Drag is also generated as a consequence of lift and surface structure of the blade. Figures 4 to 6 depict the variation of lift and drag coefficients, of the three rotor blades with the angle of attack of the rotor. Figure 4 shows the variation for NACA 62-206. An increasing trend of lift coefficient with the angle of attack up to an angle of 14° is

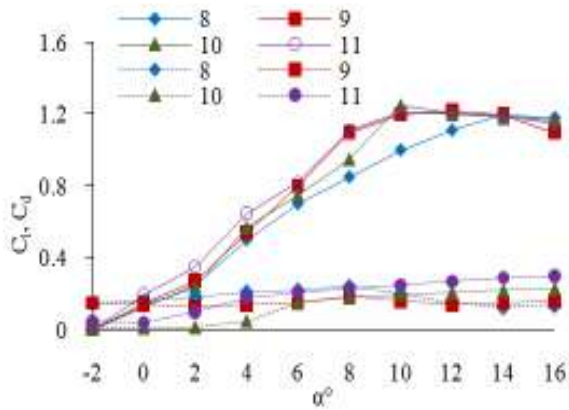


Fig. 5: Variation of lift and drag coefficient with angle of attack for NACA-4424 aerofoil

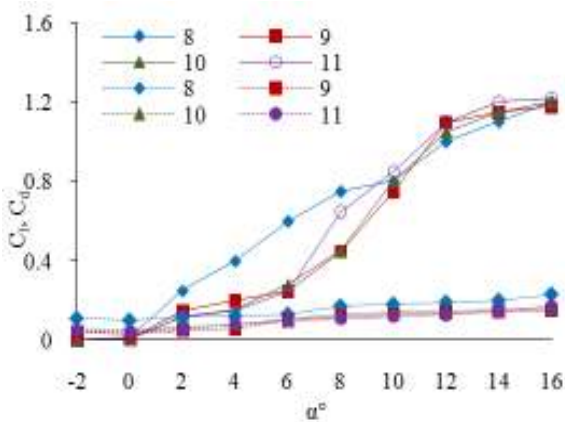


Fig. 6: Variation of lift and drag coefficient with angle of attack for NACA-23024 aerofoil

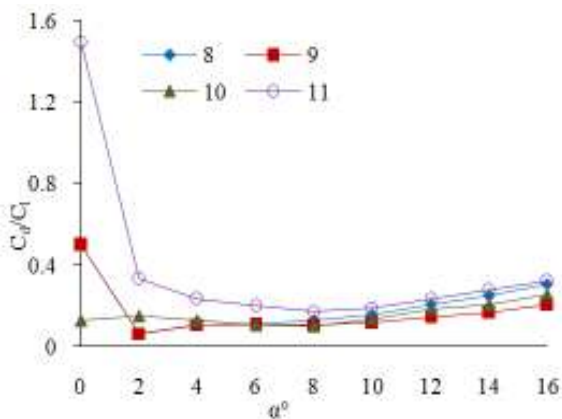


Fig. 7: Variation of ratio of lift to drag coefficient with angle of attack for NACA-62-206 aerofoil

coefficient is not zero at zero angle of attack. The zero lift coefficient lies between $\alpha = -2^\circ$ to -1° . The drag coefficient shows a polaritic change with angle of attack. The drag polar shows a minimum value between $\alpha = 0^\circ$ to 1° . The aerodynamic characteristics of other rotors having NACA4424, Fig. 5 and NACA23024, Fig. 6, as aerofoil sections also show similar trends. The lift coefficient in case of NACA 4424 rotor peaks at around 10° and lift coefficient becomes zero at around $\alpha = -1.5^\circ$. The drag is seen to be minimum near $\alpha = 0^\circ$ where after it increases along positive values of angle of attack. The variations of drag coefficient for NACA23024 are similar to NACA4424 and its lift coefficient becomes zero between $\alpha = 0$ to -1° . The angle at which maximum value of coefficient of lift is achieved by the aerofoil sections is observed to be dependent on the type of the aerofoil section; therefore that angle provides the maximum angle of attack for that kind of the wind rotor. The uncertainty analysis for the lift and drag coefficients is appended in Appendix.

In order to have good aerodynamic characteristics of the rotor, higher values of torque and power coefficient, the lift to drag ratio or C_l/C_d should be high C_d/C_l ratio should have a minimum value. Therefore besides the aerodynamic characteristic lift coefficient and drag coefficient, the ratio of these coefficients (C_d/C_l) also plays an important role in the development of power in the wind turbines. It has been shown, (Dixon and Hall, 2010) that a rotor with lower value of C_d/C_l could produce more power compared to rotors with higher values of C_d/C_l . The variation of this parameter for the three rotors at the four wind speeds (8-11 m/s) is shown in Fig. 7 to 9. In case of NACA 62-206, Fig. 7, aerofoil section this ratio decreases steeply up to $\alpha = 2^\circ$ for lower speeds followed by a gradual increase beyond that angle. At higher speeds the changes in this coefficient are small. NACA4424, Fig. 8, shows a steep decrease in this variable is seen to be up to $\alpha = 6^\circ$ thereafter a gradual increase is observed. Like NACA62-206 the variations are small at higher speeds. For the case of NACA23024, Fig. 9, the decrease of this variable is found to be steep up to $\alpha = 2^\circ$ and then unlike other aerofoils the decrease continues but gradually. A comparison of this parameter for the three types of aerofoils, Fig. 10, shows that the NACA 23024 aerofoil section generates higher values of C_d/C_l at lower angles, whereas at higher angles its values are lower than the other aerofoil sections. Other two aerofoil sections show similar variation of this parameter. Even though the minimum value of the parameter C_d/C_l is also observed to depend on the aerofoil section, but the angle at which it happens is seen to lie between 2° to 4° , which provides also the minimum angle of attack of the aerofoils. It

observed where after the lift coefficient C_l decreases. Since the aerofoil section is cambered therefore the lift

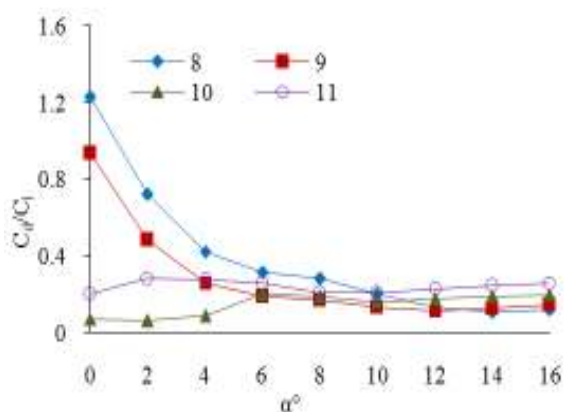


Fig. 8: Variation of ratio of lift and drag coefficient with angle of attack for NACA-4424 aerofoil

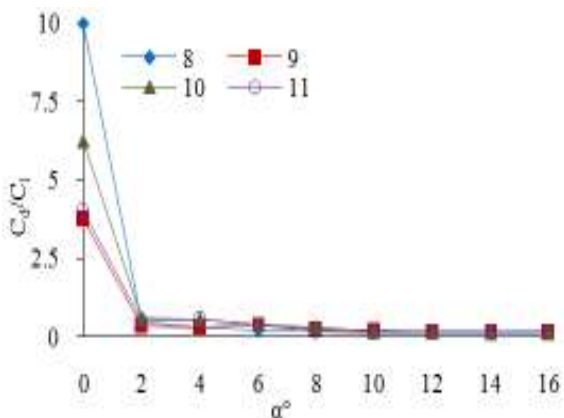


Fig. 9: Variation of ratio of lift and drag coefficient with angle of attack for NACA-23024 aerofoil

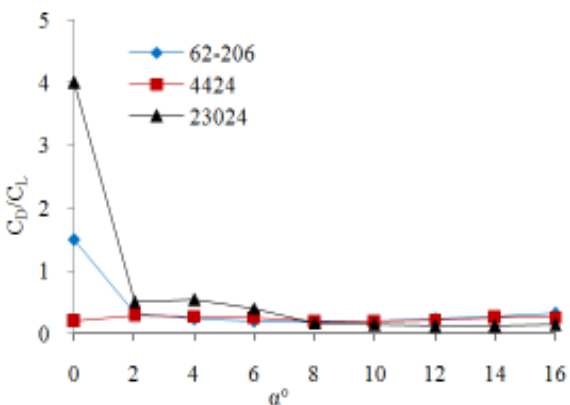


Fig. 10: Comparison of coefficient C_D/C_L of different aerofoil sections at wind speed of 11 m/s

may be added here that it is the parameters C_D/C_L rather than either C_L or C_D that has more influence of power producing capability of the wind rotor.

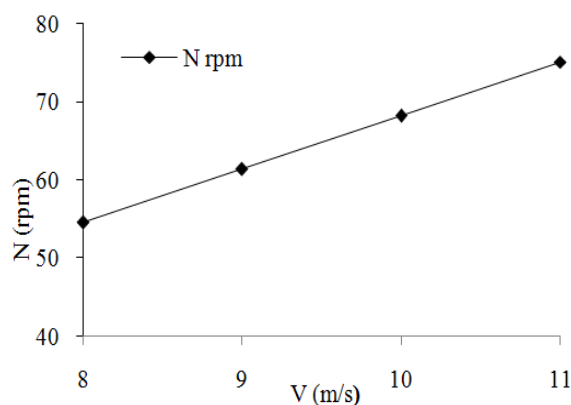


Fig. 11: Rotational characteristics of sub scale model

Rotational behavior of the rotors: The rotational behavior of the wind turbines was tested by employing three bladed rotor subscale models of rotor diameter 225 mm, rotor span 100 and 30 mm chord in a 600×600 mm blow down wind tunnel facility. The rotational speed of the subscale model was measured by a flashing stroboscope. The results of this observation for various speeds is shown in Fig. 11 where in rotational speed obtained as averaged values of the three subscale models is shown to depend on the incoming wind speed. From the rotational testing and the criterion given by Burton *et al.* (2001) a tip speed ratio of 5 was selected.

Power produced by subscale wind rotors: The variation of power produced by the three subscale wind rotors of rotor diameter 250 mm, at a uniform setting angle of 35° for free stream velocities of 8-11 m/s and at different angles of attack is given in Fig. 12. These figures demonstrate that the power produced by the wind rotor is strongly affected by wind speed, angle of attack and type of rotor aerofoil section. It is seen that the power produced by the rotor with NACA4424 aerofoil section generates higher values at angles of attack up to 12°. Beyond this value of angle of attack NACA23024 produces more power at all the wind speeds tested. Least power is observed in rotor with NACA 62-206 series aero foils sections. These observations show that NACA4424 aerofoil sectioned rotors can be used at lower wind speeds and at lower values of angles of attack whereas NACA23024 aerofoil sectioned rotors are good for higher wind speeds. Further looking back at the variation of aerodynamic coefficients it is observed that for a given wind speed and angle of attack the better performance of the rotor is related with aerofoil section with lower value of C_D/C_L coefficient at that speed and angle of

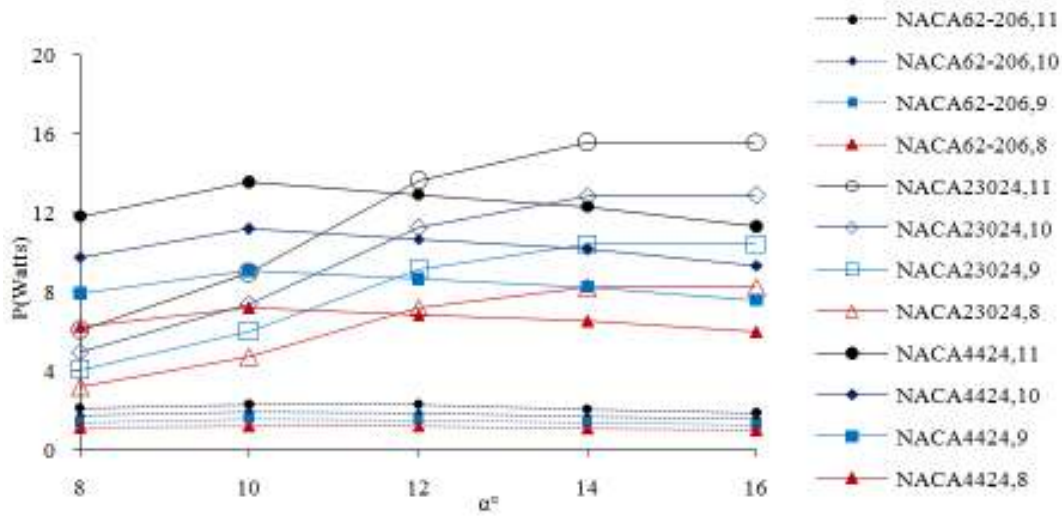


Fig. 12: Variation of power with alfa at different V for subscale model (airfoil section, velocity)

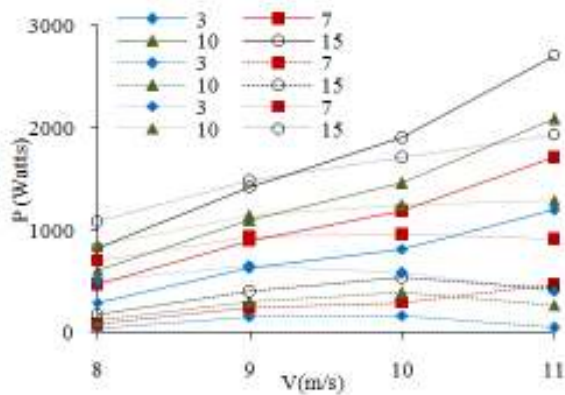


Fig. 13: Effect of setting angle on power produced at different velocities for $D = 7\text{ m}$, $\lambda = 5$ and $\alpha = 14^\circ$
 Full line: NACA23024; Dotted Line: NACA4424;
 Dashed line: NACA62-206

attack. This observation is in conformity with the results of Singh *et al.* (2012).

Parametric performance of wind turbine: The performance of a wind rotor depends on the aerodynamic behavior of the blades of the rotors which is governed by the incoming velocity of air, pitch angle of the rotor which depends on setting angle and geometric details of the rotor blade. Using the aerodynamic and rotational results of the subscale models a parametric study was carried out to find the effect of geometric and aerodynamic parameters of the wind turbine rotor on its performance. The parameters considered for performance evaluation are setting angle, diameters, tip speed ratio, taper, setting angle, diameters, tip speed ratio and taper. The output of wind

rotors is a function of wind speed. The increase in the wind speed beyond the rated value of the wind turbine causes turbine overloading and degradation of wind turbine performance. Further increase could cause blade failure. This can be overcome by using pitch controlled wind turbine rotors Ahmet and Zafer (2009) or aerodynamic break systems. In former case the fundamental technique is change in the setting angle of the rotor blade which causes the change in pitch angle that leads to changes in aerodynamic forces and moments resulting in power output changes. The setting angle of the rotors is one of important geometrical factors that affect its performance because it decides the nature in which the wind turbine cuts the incoming wind. It causes the helicoidal nature of the rotor geometry. Figure (13) demonstrates the effect of setting angle for the three rotors for a constant rotor diameter of 7 m, tip speed ratio of 5 and a fixed angle of attack of 14° . The setting angle has been varied from 3° to 15° and it is assumed that it remains constant all along the radii of the rotor. The wind speed variation is between 8 to 11 m/s. In this figure the full lines show the variation for rotor with blades of NACA 23024 airfoil section, dashed lines are for rotor with NACA4424 airfoil section whereas dotted lines are for rotor with NACA62-206 airfoil section. It is observed from the variation that the power developed by the rotor, within the speed range of 8-11 m/s, increases with the increase in the setting angle up to angle of attack of 14° . More changes are observed in rotor with NACA23024 airfoil section than the other two and rotor with NACA62-206 airfoil section shows least changes. For a setting angle it is observed that wind rotor with NACA4424 airfoil blades generates more power than

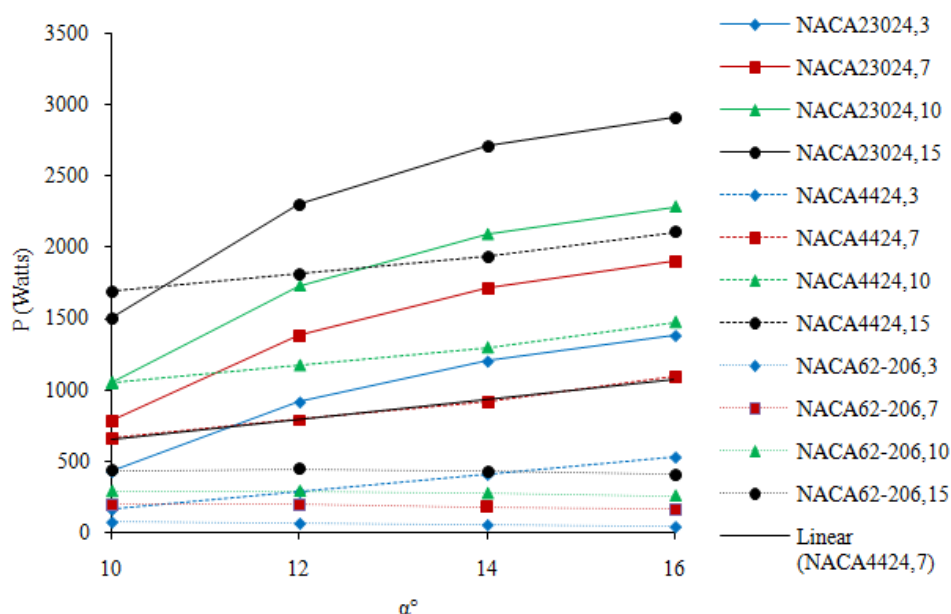


Fig. 14: Effect of setting angle on power produced at different angles of attack for $D = 7$ m, $\lambda = 5$ and $V = 11$ m/s
Full line: NACA23024; Dotted Line: NACA4424; Dashed line: NACA62-206

other two types of rotors at lower wind speeds whereas at higher wind speeds wind rotor with NACA23024 aerofoil sectioned blades produces more power. Beyond the wind speed of 10 m/s the variations depend on type of rotor. The increase in rotor with NACA62-206 aerofoil section ceases beyond the wind speed of 10 m/s for all the values of the setting angle whereas for rotor with NACA4424 this effect is felt only for lower values of setting angle. This effect is again as the consequence of the lower values of the parameter C_d/C_l for NACA23024 under the conditions of the study. At 10 m/s wind speed, at which the increment due to change in setting angle ceases for rotors with NACA4424 and NACA62-206, the power produced by rotor with NACA23024 aerofoil section at a setting angle of 15° is nearly 3.5 times that of that of rotor with NACA62-206 aerofoil section. A similar variation of power produced by the rotors with the change in angle of attack for rotor diameter of 7 m, wind speed of 11 m/s and tip speed ratio of 5 is presented in Fig. 14. In this case also the power produced by wind turbine rotor with NACA23024 aerofoil section blades produces more power at higher angles of attack for all values of setting angle whereas the rotor with NACA4424 aerofoil section blades produces higher power at lower angles of attack. The margin of angle of attack at which the rotor with NACA4424 aerofoil section generates more power decreases with the

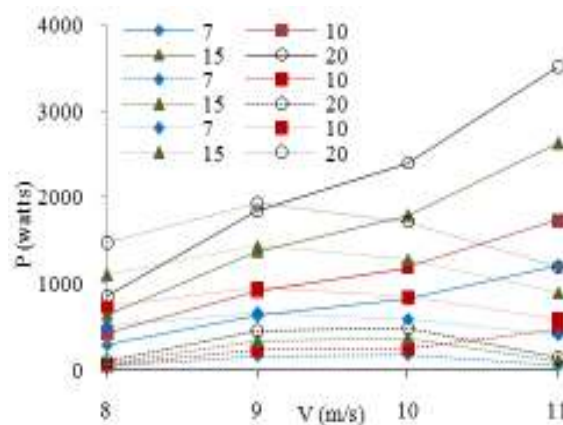


Fig. 15: Effect of rotor diameter on power produced at different velocities for $\theta = 3^\circ$, $\lambda = 5$ and $\alpha = 14^\circ$
Full line: NACA23024; Dotted Line: NACA4424; Dashed line: NACA62-206

increase in setting angle. In other words the rotor with NACA23024 aerofoil section blades would produce more power at all the angles of attack if the setting angle would be more than 15° . This may be due to the interaction of blades geometry at that setting angle with the aerodynamic characteristics of the wind rotors.

The rotor diameter is usually thought to increase the output of the wind turbine. Higher rotor diameters encounter larger winds and hence seem to increase the wind turbine power. But higher diameters are fed with

large variation in the incoming velocity as a consequence of atmospheric boundary layer. This causes consequential power losses. Figure 15 depicts the variation of the power of the three rotors for a constant angle of attack of 14° and blade setting angle of 3° for wind speeds varying between 8 to 11 m/s. The diameters have been varied from 7 to 20 m. It is observed that the power output of the wind turbine increases continuously with the increase in rotor diameters for all the rotors. For rotors with NACA 4424 blades (dotted lines) the increase in the power output is observed to decrease beyond the wind velocity of 9 m/s where as it starts dipping beyond the wind speed of 10 m/s in case of rotor with NACA-62-206 aerofoil section (dashed lines). The rotor with NACA23024 aerofoil section (full lines) shows a consistent increase with the increase in diameter of the rotor at all the wind speeds with the range at which aerodynamic testing of rotors was carried out. Further the changes of power with the change in diameters from 7 to 15 m is about 200% in rotors with NACA23024 and NACA 4424 aerofoils compared to just 100% in that of rotor with NACA62-206 aerofoil section. Also changes in the power are more in rotors with NACA23024 aerofoil section blades and least with rotor with NACA26-206 blades. Further the power produced by rotors with NACA 4424 aerofoil blades show more power produced for larger rotor diameters of rotor diameters up to wind speed of 9 m/s. The variation demonstrates that the aerofoil section NACA 4424 can be used for sites with low wind velocities. A comparison of power variation for wind rotors with NACA23024 and NACA 4424 aerofoil with angle of attack at wind speeds of 8 and 11 m/s is presented in Fig. (16). It demonstrates that the power produced by both rotors at these two speeds shows consistent increase with angle of attack. Further more changes are visible for Rotors with blades of NACA23024 aerofoil section.

The tip speed ratio of the turbine plays an important role in the development of power by the wind turbines. Dixon and Hall (2010), Koki *et al.* (2005) and Lanzafame and Massina (2007) have shown that this parameter controls the axial and rotational inflow factors a and a' which govern the velocity vector at the rotor. Further it shows the combined effect of rotational speed and wind speed for a fixed rotor diameter. A high value of tip speed ratio is usually better but the higher speeds also cause higher blade stresses and noise pollution. This parameter also governs the selection of the electrical equipment needed for energy conversion. The effect of tip speed on power produced by the three rotors is presented in Fig. 17 to 18. The tip speed ratio

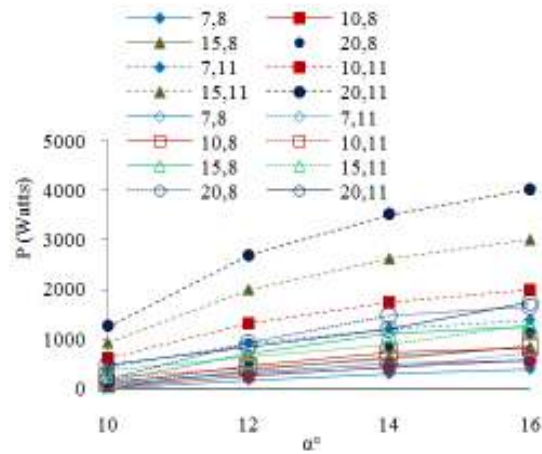


Fig. 16: Effect of rotor diameter on power produced at different angles of attack for $\theta = 3^\circ$, $\lambda = 5$ and $V = 8, 11$ m/s
Full line: NACA4424; Dotted Line: NACA23027; Dashed line: NACA62-206

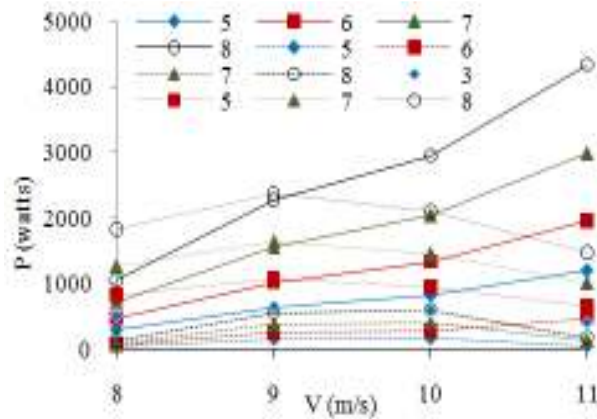


Fig. 17: Variation of power produced with different tip speed ratio for different wind speeds for $\theta = 3^\circ$, $D = 7$ m and $\alpha = 14^\circ$
Full line: NACA32024; Dotted Line: NACA4424; Dashed line: NACA62-206

has been varied from 5 to 8 while other factors were kept at constant levels. The variation of power produced by the wind rotor with a fixed value of angle of attack of 14° , setting angle of 3° and a rotor diameter of 7 m in the wind speed range of 8 to 11 m/s is shown in Fig. 17. For rotors with rotor blades of NACA4424 and NACA62-206 aerofoil section it is observed that the power output of the turbine achieves maximum value at a wind speed of 9 m/s at all the values of the tip speed ratio. Thereafter the power decreases with the increase in wind velocity. For rotor with rotor blades of NACA23024 aerofoil section the power increases rapidly up to wind speed of 9 m/s beyond which the

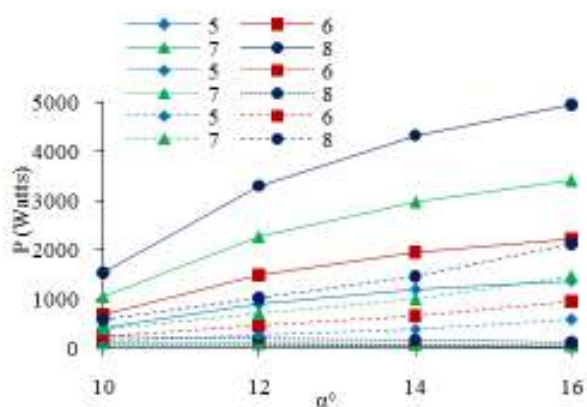


Fig. 18: Variation of power produced with different tip speed ratio for different angle of attack for $\theta = 3^\circ$, $D = 7$ m and $V = 11$ m/s
 Full line: NACA32024; Dotted Line: NACA4424;
 Dashed line: NACA62-206

increasing rate is slowed down. Again it points out that rotors with NACA4424 aerofoil sectioned blades can be used at lower wind speeds because of their geometrical thinness where as rotors with NACA23024 aerofoil section blades are good at higher speeds. It is observed from the variation of power output with tip speed that maximum power output is achieved at the tip speed ratio of 7 for most of the wind speeds in the range at which aerodynamic testing has been measured. Rotors with NACA23024 aerofoil section shows larger increments in power generation compared to the other two rotors. Rotor with NACA62-206 aerofoil section does not seem to have much effected by change of tip speed ratio. Further even for rotor with NACA23024 aerofoil section the power output is affected more at

higher wind speeds. The increase in power produced by rotor with NACA23024 is 400% compared to 200% in rotor with NACA62-206. Figure (18) shows the affect of tip speed ratio with angle of attack at a wind speed of 11 m/s for wind rotors of 7 m rotor diameter and a setting angle of 3° . More power increase is observed in rotors with NACA23024 aerofoil sectioned (full lines) than other two types of rotors. Further even the rate of increase of the power is also more compared to other two.

It can be seen that the output of a wind turbine for different rotor diameters maximizes for a wind speed. This seems that for larger rotor tips the aerodynamic phenomenon of vortex shedding occurs with a greater strength than for rotors with lesser diameters. This makes the rotor tips redundant. At these places the vortex shedding in combination with the three dimensional nature of the air flow causes larger lift losses as a consequence of the termination of aerodynamic characteristics in general and the lift coefficient in particular. This effect is exacerbated with blunt faced rotors. To decrease this effect the rounding of rotor tips or swept back rotors has been proposed by Tangler (2001). These changes involve some form of taper particularly along the leading edge of the rotor blades. Figure 19 demonstrates the use of taper in the leading edge side of the rotor. A taper of 0-33.3% has been considered. The variations are shown for a rotor of 7 m diameter with angle of attack of 14° and for a setting angle of 3° . The variations show that even though the power output of the wind turbine rotors show a decrease with the increase in the taper of the rotor blades but the decrease in not significant.

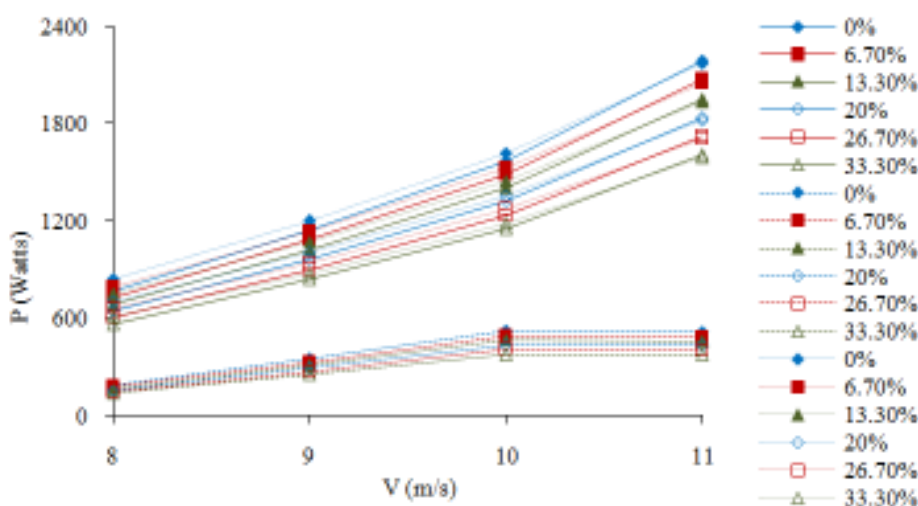


Fig. 19: Variation of power produced with different wind speeds for different taper ratios for $\theta = 3^\circ$, $D = 7$ m and $\alpha = 14^\circ$ and $\lambda = 5$. Full line: NACA32024; Dotted Line: NACA4424; Dashed line: NACA62-206

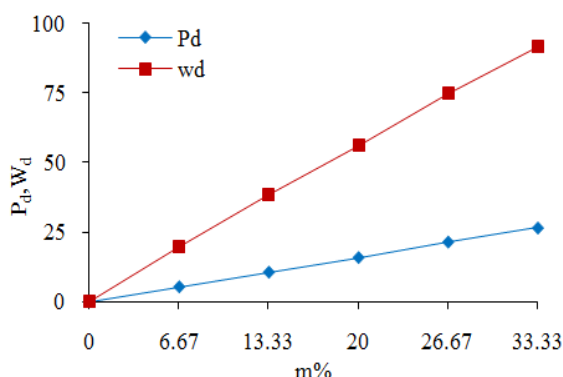


Fig. 20: Variation of power deficit and weight deficit with taper ratio for $\theta = 3^\circ$, $D = 7$ m and $\alpha = 14^\circ$ and $\lambda = 5$

Table 1: Comparison of Cp with Lanzafame and Massina (2009)

V = 4.5 m/s $\phi = 14^\circ$				
Θ°	Present investigation			Lanzafame and Massina (2009)
	NACA4424	NACA23024	NACA62-206	NACA44xx
1	0.45	0.41	0.10	0.40
4	0.34	0.38	0.08	0.31
7	0.24	0.20	0.06	0.18

Table 2: Comparison of torque (KN) with Lanzafame and Massina (2010)

D = 10 m, $\Theta = 3^\circ$, N = 72 rpm				
V	Present investigation			Lanzafame and Massina (2010)
	NACA4424	NACA23024	NACA62-206	
8	0.90	0.82	0.21	1.00
9	0.92	0.88	0.27	1.150
10	0.94	0.91	0.30	1.225
11	0.96	0.97	0.23	1.250

Therefore the decrease in power output of rotors has to be counter balanced by the decrease in overall weight of the rotors and consequently a net gain is achieved by tapering the rotors. The decrease of power and overall mass is shown in Fig. 20. In this figure the decrease in power and mass has been presented as percentage of power generated and the mass of the untapered blade. It is observed that decrease in weight overtakes the decrease in power quickly. Usually under the actual selection of taper a trade off is considered between the reduction in power and saving in dead load presented by the weight of the rotors. Besides this the tapering and curving of edges improves the aerodynamic behavior there which results in further reduction in the power deficit. The taper introduces a tradeoff between a gain in weight deficit and power deficit. It may be added here the parameters associated with the blade geometry like diameter, taper and blade shape are important for power generation. Because once

optimized a shorter and thinner bladed rotor will produce similar output as one which is not optimized and is larger in size.

The results of this investigation show similarities in the results with the works of Koki *et al.* (2005) and Lanzafame and Massina (2007). Koki *et al.* (2005) have performed the performance measurements at a wind speed of 4.5 m/s for various types and shapes of the wind turbine rotor at blade setting angles of 1° , 4° and 7° for the pitch angle value of 14° . Three types of rotors of aerofoil shapes NACA 44xx and LSOxx having no twist in plane form and NACA 44xx aerofoil with twist have been used. After investigating the performance of the rotors under these conditions it is found that small discrepancies exist between our experiment and the results. This comparison is presented in the Table 1. The differences that are found in the two results are due to the fact that the rotor in Koki *et al.* (2005) was tested in the closed jet wind tunnel.

Lanzafame and Massina (2007) conducted the investigations on a wind rotor of 10 m diameter at setting angle of 3° running at 72 rpm. A comparison with the present investigation shows more agreement with rotor having NACA23024 blade cross section. The comparison is shown in Table 2. It may be added here that the wind turbine rotors used in the present study were rectangular plane form with basic aerofoil sections without twist and any other modification. The differences in the values of Cp can hence be attributed to geometrical difference.

CONCLUSION

This study utilizes the mathematical formulation based on blade element-momentum theory of the wind rotors that can be applied to variety of wind rotors with variations in all the aerodynamic and geometrical parameters that affect the performance of these rotors. This study shows that the power generated by a wind rotor changes with the change in wind speed, angle of attack and the setting angle. It also shows that the changes in diameter and tip speed ratio become insignificant beyond a wind speed of 9 m/s. In the given range of wind speeds the change in the power produced by rotor with NACA23024 with changes in diameter and setting angle is seen to be 4 times more than that with NACA62-206 aerofoil. Further the taper introduces more mass deficit gain than a power deficit. Most importantly it is obvious from the results that wind rotors with blades made out of NACA4424 aerofoil section can be used at lower wind speeds compared to the NACA23024 which has to be used for higher wind speeds. Intended future studies will consider the effect of changing the airfoil shape along

the blade span with the use of special types other than those from the NACA families. Wind velocity analysis shall contain additional components due to turbulence, which needs large statistical data collection of wind fluctuations at the specific site.

ACKNOWLEDGMENT

The authors extend their appreciation to the Deanship of Scientific Research at King Saud University for funding the work through the research group project No RGP-VPP-036.

NOMENCLATURE

- a : Axial induction factor
- a_t : Tangential induction factor
- c : Chord (m)
- C_d : Drag coefficient
- C_l : Lift Coefficient
- D : Diameter of rotor
- d : Rotor height (m)
- d_D : Elemental drag force (N)
- d_N : Elemental normal force (N)
- d_T : Elemental tangential force (N)
- d_R : Elemental resultant force (N)
- F : Tip loss factor
- m_d : Mass deficit of rotor blades (kg)
- m : Slop of blade taper (m)
- N : Rotational speed of the rotor (rps)
- P : Power (W)
- P_d : Power Deficit
- r : Radius (m)
- R_h : Rotor hub radius (m)
- R_m : Rotor mean radius (m)
- R_t : Rotor tip radius (m)
- s : Pitch (m)
- V₀ : Free stream velocity (m/s)
- V₁ : Relative velocity at the rotor aerofoil (m/s)
- Z : Number of blades
- α : Angle of attack (blade incidence angle) (°)
- θ : Blade setting angle (°)
- λ : Tip speed ratio = ωD/V₀
- ρ : Density of air (kg/m³)
- φ : Pitch angle (°)
- ω : Angular speed (radians/sec)

Appendix: Uncertainty analysis

The uncertainty analysis of a variable R which depends many independent variables X_i (i = 1-n) in the following manner:

$$R = f(X_1^a, X_2^b, \dots, X_n^m)$$

Is given as:

$$\frac{U_R}{R} = \pm \left[\left(a \frac{U_{X_1}}{X_1} \right)^2 + \left(b \frac{U_{X_2}}{X_2} \right)^2 + \left(c \frac{U_{X_3}}{X_3} \right)^2 + \dots + \left(m \frac{U_{X_n}}{X_n} \right)^2 \right]^{\frac{1}{2}}$$

Uncertainty of Mean Velocity:

Using Bernoulli's equation the mean velocity at a point is given as:

$$V = \sqrt{\frac{2 * g * R * T_a * \Delta H * \rho_w}{P_a}}$$

The values of different quantities and their uncertainties are:

ΔH = 6.5 mm of water; U_H = ±0.05 mm of water

T_a = 33°C; U_T = ±0.5°C

ρ_a = 764.5 mm of Hg; U_{pa} = 0.15 mm Hg

ρ_w = 1000 kg/m³; U_{ρw} = 0.01 kg/m³

Keeping R (gas constant of air) and g (acceleration due to gravity) without any uncertainty

Therefore the uncertainty of mean velocity is given as:

$$\frac{U_V}{V} = \pm \left\{ \left(\frac{1}{2} * \frac{U_{T_a}}{T_a} \right)^2 + \left(\frac{1}{2} * \frac{U_{P_a}}{P_a} \right)^2 + \left(\frac{1}{2} * \frac{U_{\Delta H}}{\Delta H} \right)^2 + \left(\frac{1}{2} * \frac{U_{\rho_w}}{\rho_w} \right)^2 \right\}^{\frac{1}{2}}$$

$$\frac{U_V}{V} = \pm \left\{ \left(\frac{1}{2} * \frac{0.5}{33} \right)^2 + \left(\frac{1}{2} * \frac{0.15}{760} \right)^2 + \left(\frac{1}{2} * \frac{0.05}{6.5} \right)^2 + \left(\frac{1}{2} * \frac{0.01}{1000} \right)^2 \right\}^{\frac{1}{2}}$$

$$\frac{U_V}{V} = 0.0085 = 0.85\%$$

Using the similar technique the uncertainties for the coefficients of lift and drag were also evaluated as under:

$$C_L = \frac{L}{0.5 * \rho * V^2 * c * l} \text{ and } C_D = \frac{D}{0.5 * \rho * V^2 * c * l}$$

The repeated measurements and the catalogue of the wind tunnel balance yielded:

$$\frac{U_L}{L} = \pm 0.002 \text{ and } \frac{U_D}{D} = \pm 0.005$$

Defining density as $\rho = \frac{P}{RT}$ and evaluating its uncertainty yield

$$\frac{U_\rho}{\rho} = \pm 0.0017$$

Further uncertainty of chord and span were evaluated as:

$$\frac{U_c}{c} = \pm 0.008 \text{ and } \frac{U_l}{l} = \pm 0.0025$$

Therefore the uncertainty of coefficient of lift and drag yield the following results:

$$\frac{U_{C_L}}{L} = \pm 0.0123 \text{ and } \frac{U_{C_D}}{D} = \pm 0.042$$

REFERENCES

- Ahmet, S.Y. and O. Zafer, 2009. Pitch angle control in wind turbines above the rated wind speeds by multi-layer perception and radial basis function neural networks. Expert Syst. Appl., 36: 9767-9775.
- Ameku, K., B.M. Nagai and J.N. Roy, 2008. Design of a 3 KW wind turbine with thin airfoil blades. Exp. Therm. Fluid Sci., 32: 1723-1730.
- Baskut, O., O. Ozgener and L. Ozgener, 2010. Effects of meteorological variables on exergetic efficiency of wind turbine power plant. Renew. S. Energy Rev., DOI: 10.1016.

- Buhl Jr., L. Marshall, 2005. A new empirical relationship between thrust coefficient and induction factor for the turbulent windmill state. Technical Report NREL/TP-500-36834, August, 2005.
- Burton, T., D. Sharpe, N. Jenkins and E. Bossanyi, 2001. Wind Energy Handbook. John Wiley and Sons, New York.
- Cameron, A., 2011. Flying under the radar. Wind Technol. Renew. Energy World, pp: 4-6.
- Dixon, S.L. and C.A. Hall, 2010. Fluid Mechanics and Thermodynamics of Turbomachinery. 6th Edn., Butterworth-Heinemann, Elsevier, UK.
- Fujisawa, N. and F. Goto, 1994. Experimental study on the aerodynamic performance of Sarvonius rotor. ASME J. Sol. Energ. Eng., 115: 148-152.
- Gigue`re, P. and M.S. Selig, 1999. Design of a Tapered and Twisted Blade for the NREL Combined Experiment Rotor. National Renewable Energy Laboratory, Golden, CO.
- Gigue`re, P., M.S. Selig and J.L. Tangler, 1999. Blade design trade-offs using low-lift airfoil for stall-regulated HAWTs. National Renewable Energy Laboratory, Golden, CO.
- Glauert, H., 1926. The Elements of Airfoil and Airscrew Theory. Cambridge University Press, Cambridge.
- Hansen, M.O.L., 2000. Documentation of code and airfoil data used for the NREL 10-m wind turbine. ROTABEM-DTU, November 2000.
- Koki, K., T. Hiroshi, S. Jun, I. Hiroshi, K. Takashi and T. Masato, 2005. Theoretical and experimental study on the aerodynamic characteristics of a horizontal axis wind turbine. Energ., 30(11-12): 2089-2100.
- Lanzafame, R. and M. Messina, 2007. Fluid dynamics wind turbine design: Critical analysis, optimization and application of BEM theory. Energ., 32(14): 2291-2305.
- Lanzafame, R. and M. Messina, 2009. Optimal wind turbine design to maximize energy production. JPE 679, IMechE, Proc. IMechE Part A: J. Power Energ., 223(2): 93-101.
- Lindenburg, C., 2003. Investigation into Rotor Blade Aerodynamics. ECN-C-03-025.
- Moffat, R.J., 1985. Using uncertainty analysis in the planning of an experiment. J. Fluid. Eng., 107: 173-176.
- Ozgener, O., 2005. A review of blade structures of SWTs in the Aegean region and performance analysis. Renew. S. Energy Rev., 9: 85-99.
- Ozgener, O., 2006. A Small Wind Turbine System (SWTS) application and its performance analysis. Energ. Convers. Manage., 47: 1326-1337.
- Ozgener, O. and L. Ozgener, 2007. Exergy and reliability analysis of wind turbine systems: A case study. Renew. S. Energy Rev., 11: 1811-1826.
- Pinto, R.T., 2011. Standards for the sea. Wind Technol. Renew. Energy World, pp: 20-22.
- Renewable Energy World, 2011. Gathering Momentum., 14(6): 7.
- Rope, K., I. Dincer and G.F. Naterer, 2010. Energy and exergy efficiency comparison of horizontal and vertical axis wind turbines. Renew. Energy, 35: 2102-2113.
- Sahin, A.D., I. Dincer and M.A. Rosen, 2006. Thermodynamic analysis of wind energy. Int. J. Energy Res., 30: 553-566.
- Shimizu, Y., M. Takada and J. Sakata, 1998. Development of a high-performance cross flow turbine. Trans. JSME, 625: 202-207.
- Singh, R.K., M.R. Ahmed, M.A. Zullah and Y.H. Lee, 2012. Design of a low Reynolds number airfoil for small horizontal axis wind turbines. Renew. Energ., 42: 66-76.
- Tangler, J.L., 2000. The evolution of rotor and blade design. NREL/CP-500-28410.
- Varol, A., C. Ilkilic and Y. Varol 2001. Increasing the efficiency of wind turbines. J. Wind Engg Ind. Aerodynamics, 89: 809-815.